5

Case Study: The Pelican Prototype Robot

The purpose of this chapter is twofold: first, to present in detail the model of the experimental robot arm of the Robotics lab. from the CICESE Research Center, Mexico. Second, to review the topics studied in the previous chapters and to discuss, through this case study, the topics of direct kinematics and inverse kinematics, which are fundamental in determining robot models.

For the Pelican, we derive the full dynamic model of the prototype; in particular, we present the numerical values of all the parameters such as mass, inertias, lengths to centers of mass, *etc.* This is used throughout the rest of the book in numerous examples to illustrate the performance of the controllers that we study. We emphasize that *all* of these examples contain *experimentation* results.

Thus, the chapter is organized in the following sections:

- direct kinematics;
- inverse kinematics;
- dynamic model;
- properties of the dynamic model;
- reference trajectories.

For analytical purposes, further on, we refer to Figure 5.2, which represents the prototype schematically. As is obvious from this figure, the prototype is a planar arm with two links connected through revolute joints, *i.e.* it possesses 2 DOF. The links are driven by two electrical motors located at the "shoulder" (base) and at the "elbow". This is a direct-drive mechanism, *i.e.* the axes of the motors are connected directly to the links without gears or belts.

The manipulator arm consists of two rigid links of lengths l_1 and l_2, masses m_1 and m_2 respectively. The robot moves about on the plane x–y as is illustrated in Figure 5.2. The distances from the rotating axes to the centers of mass are denoted by l_{c1} and l_{c2} for links 1 and 2, respectively. Finally, I_1 and

Figure 5.1. Pelican: experimental robot arm at CICESE, Robotics lab.
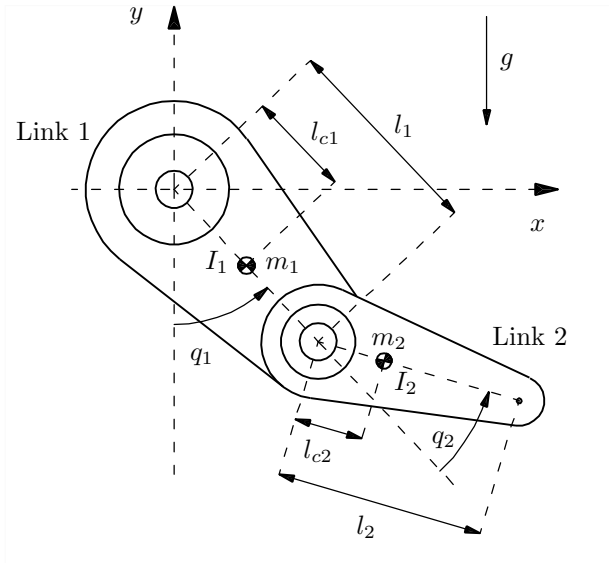
Figure 5.2. Diagram of the 2-DOF Pelican prototype robot

I_2 denote the moments of inertia of the links with respect to the axes that pass through the respective centers of mass and are parallel to the axis x. The degrees of freedom are associated with the angle q_1, which is measured from the vertical position, and q_2, which is measured relative to the extension of the first link toward the second link, both being positive counterclockwise. The vector of joint positions $\boldsymbol{q}$ is defined as

$$\boldsymbol{q} = [q_1 \quad q_2]^T.$$

The meaning of the diverse constant parameters involved as well as their numerical values are summarized in Table 5.1.

Table 5.1. Physical parameters of Pelican robot arm

Description	Notation	Value	Units
Length of Link 1	l_1	0.26	m
Length of Link 2	l_2	0.26	m
Distance to the center of mass (Link 1)	l_{c1}	0.0983	m
Distance to the center of mass (Link 2)	l_{c2}	0.0229	m
Mass of Link 1	m_1	6.5225	kg
Mass of Link 2	m_2	2.0458	kg
Inertia rel. to center of mass (Link 1)	I_1	0.1213	kg m^2
Inertia rel. to center of mass (Link 2)	I_2	0.0116	kg m^2
Gravity acceleration	g	9.81	m/s^2

5.1 Direct Kinematics

The problem of direct kinematics for robot manipulators is formulated as follows. Consider a robot manipulator of n degrees-of-freedom placed on a fixed surface. Define a reference frame also fixed at some point on this surface. This reference frame is commonly referred to as 'base reference frame'. The problem of deriving the direct kinematic model of the robot consists in expressing the position and orientation (when the latter makes sense) of a reference frame fixed to the end of the last link of the robot, referred to the base reference frame in terms of the joint coordinates of the robot. The solution to the so-formulated problem from a mathematical viewpoint, reduces to solving a geometrical problem which always has a closed-form solution.

Regarding the Pelican robot, we start by defining the reference frame of base as a Cartesian coordinated system in two dimensions with its origin located exactly on the first joint of the robot, as is illustrated in Figure 5.2. The Cartesian coordinates x and y determine the position of the tip of the second link with respect to the base reference frame. Notice that for the present case study of a 2-DOF system, the orientation of the end-effector of the arm makes no sense. One can clearly appreciate that both Cartesian coordinates, x and

y, depend on the joint coordinates q_1 and q_2. Precisely it is this correlation that defines the direct kinematic model,

$$\begin{bmatrix} x \\ y \end{bmatrix} = \boldsymbol{\varphi}(q_1, q_2),$$

where $\boldsymbol{\varphi} : \mathbb{R}^2 \to \mathbb{R}^2$.

For the case of this robot with 2 DOF, it is immediate to verify that the direct kinematic model is given by

$$x = l_1\sin(q_1) + l_2\sin(q_1 + q_2)$$
$$y = -l_1\cos(q_1) - l_2\cos(q_1 + q_2).$$

From this model is obtained: the following relation between the velocities

$$\begin{bmatrix} \dot{x} \\ \dot{y} \end{bmatrix} = \begin{bmatrix} l_1\cos(q_1) + l_2\cos(q_1 + q_2) & l_2\cos(q_1 + q_2) \\ l_1\sin(q_1) + l_2\sin(q_1 + q_2) & l_2\sin(q_1 + q_2) \end{bmatrix} \begin{bmatrix} \dot{q}_1 \\ \dot{q}_2 \end{bmatrix}$$
$$= J(\boldsymbol{q}) \begin{bmatrix} \dot{q}_1 \\ \dot{q}_2 \end{bmatrix}$$

where $J(\boldsymbol{q}) = \dfrac{\partial \boldsymbol{\varphi}(\boldsymbol{q})}{\partial \boldsymbol{q}} \in \mathbb{R}^{2 \times 2}$ is called the analytical Jacobian matrix or simply, the Jacobian of the robot. Clearly, the following relationship between accelerations also holds,

$$\begin{bmatrix} \ddot{x} \\ \ddot{y} \end{bmatrix} = \begin{bmatrix} \dfrac{d}{dt}J(\boldsymbol{q}) \end{bmatrix} \begin{bmatrix} \dot{q}_1 \\ \dot{q}_2 \end{bmatrix} + J(\boldsymbol{q}) \begin{bmatrix} \ddot{q}_1 \\ \ddot{q}_2 \end{bmatrix}.$$

The procedure by which one computes the derivatives of the Jacobian and thereby obtains expressions for the velocities in Cartesian coordinates, is called differential kinematics. This topic is not studied in more detail in this textbook since *we* do not use it for control.
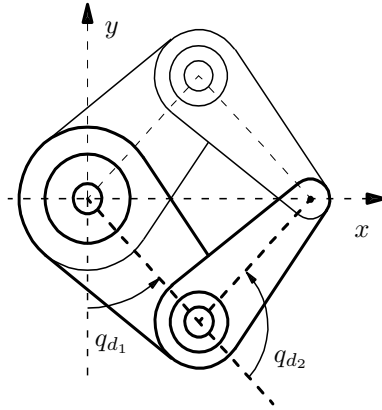
5.2 Inverse Kinematics

The inverse kinematic model of robot manipulators is of great importance from a practical viewpoint. This model allows us to obtain the joint positions $\boldsymbol{q}$ in terms of the position and orientation of the end-effector of the last link referred to the base reference frame. For the case of the Pelican prototype robot, the inverse kinematic model has the form

$$\begin{bmatrix} q_1 \\ q_2 \end{bmatrix} = \boldsymbol{\varphi}^{-1}(x, y)$$

where $\boldsymbol{\varphi}^{-1} : \Theta \to \mathbb{R}^2$ and $\Theta \subseteq \mathbb{R}^2$.

The derivation of the inverse kinematic model is in general rather complex and, in contrast to the direct kinematics problem, it may have multiple solutions or no solution at all! The first case is illustrated in Figure 5.3. Notice that for the same position (in Cartesian coordinates x, y) of the arm tip there exist two possible configurations of the links, *i.e.* two possible values for $\boldsymbol{q}$.

Figure 5.3. Two solutions to the inverse kinematics problem

So we see that even for this relatively simple robot configuration there exist more than one solution to the inverse kinematics problem.

The practical interest of the inverse kinematic model relies on its utility to define desired joint positions $\boldsymbol{q}_d = [q_{d_1} \quad q_{d_2}]^T$ from specified desired positions x_d and y_d for the robot's end-effector. Indeed, note that physically, it is more intuitive to specify a task for a robot in end-effector coordinates so that interest in the inverse kinematics problem increases with the complexity of the manipulator (number of degrees of freedom).

Thus, let us now make our this discussion more precise by analytically computing the solutions $\begin{bmatrix} q_{d_1} \\ q_{d_2} \end{bmatrix} = \boldsymbol{\varphi}^{-1}(x_d, y_d)$. The desired joint positions $\boldsymbol{q}_d$ can be computed using tedious but simple trigonometric manipulations to obtain

$$q_{d_1} = \tan^{-1}\left(\frac{x_d}{-y_d}\right) - \tan^{-1}\left(\frac{l_2 \sin(q_{d_2})}{l_1 + l_2 \cos(q_{d_2})}\right)$$

$$q_{d_2} = \cos^{-1}\left(\frac{x_d^2 + y_d^2 - l_1^2 - l_2^2}{2 l_1 l_2}\right) .$$

The desired joint velocities and accelerations may be obtained via the *differential* kinematics[1] and its time derivative. In doing this one must keep in mind that the expressions obtained are valid only as long as the robot does not "fall" into a singular configuration, that is, as long as the Jacobian $J(\boldsymbol{q}_d)$ is square and nonsingular. These expressions are

$$\begin{bmatrix} \dot{q}_{d_1} \\ \dot{q}_{d_2} \end{bmatrix} = J^{-1}(\boldsymbol{q}_d) \begin{bmatrix} \dot{x}_d \\ \dot{y}_d \end{bmatrix}$$

$$\begin{bmatrix} \ddot{q}_{d_1} \\ \ddot{q}_{d_2} \end{bmatrix} = \underbrace{-J^{-1}(\boldsymbol{q}_d) \left[\frac{d}{dt} J(\boldsymbol{q}_d) \right] J^{-1}(\boldsymbol{q}_d) \begin{bmatrix} \dot{x}_d \\ \dot{y}_d \end{bmatrix}}_{\frac{d}{dt} \left[J^{-1}(\boldsymbol{q}_d) \right]} + J^{-1}(\boldsymbol{q}_d) \begin{bmatrix} \ddot{x}_d \\ \ddot{y}_d \end{bmatrix}$$

where $J^{-1}(\boldsymbol{q}_d)$ and $\frac{d}{dt}[J(\boldsymbol{q}_d)]$ denote the inverse of the Jacobian matrix and its time derivative respectively, evaluated at $\boldsymbol{q} = \boldsymbol{q}_d$. These are given by

$$J^{-1}(\boldsymbol{q}_d) = \begin{bmatrix} \dfrac{S_{12}}{l_1 S_2} & -\dfrac{C_{12}}{l_1 S_2} \\ \dfrac{-l_1 S_1 - l_2 S_{12}}{l_1 l_2 S_2} & \dfrac{l_1 C_1 + l_2 C_{12}}{l_1 l_2 S_2} \end{bmatrix},$$

and

$$\frac{d}{dt}[J(\boldsymbol{q}_d)] = \begin{bmatrix} -l_1 S_1 \dot{q}_{d_1} - l_2 S_{12}(\dot{q}_{d_1} + \dot{q}_{d_2}) & -l_2 S_{12}(\dot{q}_{d_1} + \dot{q}_{d_2}) \\ l_1 C_1 \dot{q}_{d_1} + l_2 C_{12}(\dot{q}_{d_1} + \dot{q}_{d_2}) & l_2 C_{12}(\dot{q}_{d_1} + \dot{q}_{d_2}) \end{bmatrix},$$

where, for simplicity, we have used the notation $S_1 = \sin(q_{d_1})$, $S_2 = \sin(q_{d_2})$, $C_1 = \cos(q_{d_1})$, $S_{12} = \sin(q_{d_1} + q_{d_2})$, $C_{12} = \cos(q_{d_1} + q_{d_2})$.

Notice that the term S_2 appears in the denominator of all terms in $J(\boldsymbol{q})^{-1}$ hence, $q_{d_2} = n\pi$, with $n \in \{0, 1, 2, \ldots\}$ and any q_{d_1} also correspond to singular configurations. Physically, these configurations (for any valid n) represent the second link being completely extended or bent over the first, as is illustrated in Figure 5.4. Typically, singular configurations are those in which the end-effector of the robot is located at the physical boundary of the workspace (that is, the physical space that the end-effector can reach). For instance, the singular configuration corresponding to being stretched out corresponds to the end-effector being placed anywhere on the circumference of radius $l_1 + l_2$, which is the boundary of the robot's workspace. As for Figure 5.4 the origin of the coordinates frame constitute another point of this boundary.

Having illustrated the inverse kinematics problem through the planar manipulator of Figure 5.2 we stop our study of inverse kinematics since it is

---

[1] For a definition and a detailed treatment of differential kinematics see the book (Sciavicco, Siciliano 2000) —*cf.* Bibliography at the end of Chapter 1.
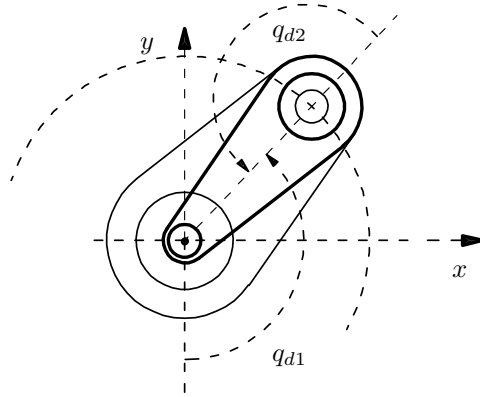
Figure 5.4. "Bent-over" singular configuration

beyond the scope of this text. However, we stress that what we have seen in the previous paragraphs extends in general.

In summary, we can say that if the control is based on the Cartesian coordinates of the end-effector, when designing the desired task for a manipulator's end-effector one must take special care that the configurations for the latter do not yield singular configurations. Concerning the controllers studied in this textbook, the reader should not worry about singular configurations since the Jacobian is not used at all: the reference trajectories are given in joint coordinates and we measure joint coordinates. This is what is called "control in joint space".

Thus, we leave the topic of kinematics to pass to the stage of modeling that is more relevant for control, *from the viewpoint of this* textbook, *i.e.* dynamics.

5.3 Dynamic Model

In this section we derive the Lagrangian equations for the CICESE prototype shown in Figure 5.1 and then we present in detail, useful bounds on the matrices of inertia, centrifugal and Coriolis forces, and on the vector of gravitational torques. Certainly, the model that we derive here applies to any planar manipulator following the same convention of coordinates as for our prototype.

5.3.1 Lagrangian Equations

Consider the 2-DOF robot manipulator shown in Figure 5.2. As we have learned from Chapter 3, to derive the Lagrangian dynamics we start by writing

the kinetic energy function, $\mathcal{K}(\boldsymbol{q}, \dot{\boldsymbol{q}})$, defined in (3.15). For this manipulator, it may be decomposed into the sum of the two parts:

- the product of half the mass times the square of the speed of the center of mass; plus
- the product of half its moment of inertia (referred to the center of mass) times the square of its angular velocity (referred to the center of mass).

That is, we have $\mathcal{K}(\boldsymbol{q}, \dot{\boldsymbol{q}}) = \mathcal{K}_1(\boldsymbol{q}, \dot{\boldsymbol{q}}) + \mathcal{K}_2(\boldsymbol{q}, \dot{\boldsymbol{q}})$ where $\mathcal{K}_1(\boldsymbol{q}, \dot{\boldsymbol{q}})$ and $\mathcal{K}_2(\boldsymbol{q}, \dot{\boldsymbol{q}})$ are the kinetic energies associated with the masses m_1 and m_2 respectively. Let us now develop in more detail, the corresponding mathematical expressions. To that end, we first observe that the coordinates of the center of mass of link 1, expressed on the plane x–y, are

$$x_1 = l_{c1}\sin(q_1)$$
$$y_1 = -l_{c1}\cos(q_1)\,.$$

The velocity vector $\boldsymbol{v}_1$ of the center of mass of such a link is then,

$$\boldsymbol{v}_1 = \begin{bmatrix} \dot{x}_1 \\ \dot{y}_1 \end{bmatrix} = \begin{bmatrix} l_{c1}\cos(q_1)\dot{q}_1 \\ l_{c1}\sin(q_1)\dot{q}_1 \end{bmatrix}\,.$$

Therefore, the speed squared, $\|\boldsymbol{v}_1\|^2 = \boldsymbol{v}_1^T\boldsymbol{v}_1$, of the center of mass becomes

$$\boldsymbol{v}_1^T\boldsymbol{v}_1 = l_{c1}^2\dot{q}_1^2\,.$$

Finally, the kinetic energy corresponding to the motion of link 1 can be obtained as

$$\mathcal{K}_1(\boldsymbol{q}, \dot{\boldsymbol{q}}) = \frac{1}{2}m_1\boldsymbol{v}_1^T\boldsymbol{v}_1 + \frac{1}{2}I_1\dot{q}_1^2$$
$$= \frac{1}{2}m_1 l_{c1}^2\dot{q}_1^2 + \frac{1}{2}I_1\dot{q}_1^2\,. \tag{5.1}$$

On the other hand, the coordinates of the center of mass of link 2, expressed on the plane x–y are

$$x_2 = l_1\sin(q_1) + l_{c2}\sin(q_1 + q_2)$$
$$y_2 = -l_1\cos(q_1) - l_{c2}\cos(q_1 + q_2)\,.$$

Consequently, the velocity vector $\boldsymbol{v}_2$ of the center of mass of such a link is

$$\boldsymbol{v}_2 = \begin{bmatrix} \dot{x}_2 \\ \dot{y}_2 \end{bmatrix}$$
$$= \begin{bmatrix} l_1\cos(q_1)\dot{q}_1 + l_{c2}\cos(q_1 + q_2)[\dot{q}_1 + \dot{q}_2] \\ l_1\sin(q_1)\dot{q}_1 + l_{c2}\sin(q_1 + q_2)[\dot{q}_1 + \dot{q}_2] \end{bmatrix}\,.$$

Therefore, using the trigonometric identities $\cos(\theta)^2 + \sin(\theta)^2 = 1$ and $\sin(q_1)\sin(q_1 + q_2) + \cos(q_1)\cos(q_1 + q_2) = \cos(q_2)$ we conclude that the speed squared, $\|v_2\|^2 = v_2^T v_2$, of the center of mass of link 2 satisfies

$$v_2^T v_2 = l_1^2 \dot{q}_1^2 + l_{c2}^2 \left[\dot{q}_1^2 + 2\dot{q}_1 \dot{q}_2 + \dot{q}_2^2\right] + 2l_1 l_{c2} \left[\dot{q}_1^2 + \dot{q}_1 \dot{q}_2\right] \cos(q_2)$$

which implies that

$$\begin{aligned}
\mathcal{K}_2(q, \dot{q}) &= \frac{1}{2} m_2 v_2^T v_2 + \frac{1}{2} I_2 [\dot{q}_1 + \dot{q}_2]^2 \\
&= \frac{m_2}{2} l_1^2 \dot{q}_1^2 + \frac{m_2}{2} l_{c2}^2 \left[\dot{q}_1^2 + 2\dot{q}_1 \dot{q}_2 + \dot{q}_2^2\right] \\
&\quad + m_2 l_1 l_{c2} \left[\dot{q}_1^2 + \dot{q}_1 \dot{q}_2\right] \cos(q_2) \\
&\quad + \frac{1}{2} I_2 [\dot{q}_1 + \dot{q}_2]^2.
\end{aligned}$$

Similarly, the potential energy may be decomposed as the sum of the terms $\mathcal{U}(q) = \mathcal{U}_1(q) + \mathcal{U}_2(q)$, where $\mathcal{U}_1(q)$ and $\mathcal{U}_2(q)$ are the potential energies associated with the masses m_1 and m_2 respectively. Thus, assuming that the potential energy is zero at $y = 0$, we obtain

$$\mathcal{U}_1(q) = -m_1 l_{c1} g \, \cos(q_1)$$

and

$$\mathcal{U}_2(q) = -m_2 l_1 g \, \cos(q_1) - m_2 l_{c2} g \, \cos(q_1 + q_2). \tag{5.2}$$

From Equations (5.1)–(5.2) we obtain the Lagrangian as

$$\begin{aligned}
\mathcal{L}(q, \dot{q}) &= \mathcal{K}(q, \dot{q}) - \mathcal{U}(q) \\
&= \mathcal{K}_1(q, \dot{q}) + \mathcal{K}_2(q, \dot{q}) - \mathcal{U}_1(q) - \mathcal{U}_2(q) \\
&= \frac{1}{2} [m_1 l_{c1}^2 + m_2 l_1^2] \dot{q}_1^2 + \frac{1}{2} m_2 l_{c2}^2 \left[\dot{q}_1^2 + 2\dot{q}_1 \dot{q}_2 + \dot{q}_2^2\right] \\
&\quad + m_2 l_1 l_{c2} \, \cos(q_2) \left[\dot{q}_1^2 + \dot{q}_1 \dot{q}_2\right] \\
&\quad + [m_1 l_{c1} + m_2 l_1] g \, \cos(q_1) \\
&\quad + m_2 g l_{c2} \, \cos(q_1 + q_2) \\
&\quad + \frac{1}{2} I_1 \dot{q}_1^2 + \frac{1}{2} I_2 [\dot{q}_1 + \dot{q}_2]^2.
\end{aligned}$$

From this last equation we obtain the following expression:

$$\begin{aligned}
\frac{\partial \mathcal{L}}{\partial \dot{q}_1} &= [m_1 l_{c1}^2 + m_2 l_1^2] \dot{q}_1 + m_2 l_{c2}^2 \dot{q}_1 + m_2 l_{c2}^2 \dot{q}_2 \\
&\quad + 2m_2 l_1 l_{c2} \, \cos(q_2) \dot{q}_1 + m_2 l_1 l_{c2} \, \cos(q_2) \dot{q}_2 \\
&\quad + I_1 \dot{q}_1 + I_2 [\dot{q}_1 + \dot{q}_2].
\end{aligned}$$

$$\frac{d}{dt}\left[\frac{\partial \mathcal{L}}{\partial \dot{q}_1}\right] = \left[m_1 l_{c1}^2 + m_2 l_1^2 + m_2 l_{c2}^2 + 2m_2 l_1 l_{c2} \cos(q_2)\right]\ddot{q}_1$$
$$+ \left[m_2 l_{c2}^2 + m_2 l_1 l_{c2} \cos(q_2)\right]\ddot{q}_2$$
$$- 2m_2 l_1 l_{c2}\sin(q_2)\dot{q}_1\dot{q}_2 - m_2 l_1 l_{c2}\sin(q_2)\dot{q}_2^2$$
$$+ I_1\ddot{q}_1 + I_2[\ddot{q}_1 + \ddot{q}_2].$$

$$\frac{\partial \mathcal{L}}{\partial q_1} = -[m_1 l_{c1} + m_2 l_1]g\,\sin(q_1) - m_2 g l_{c2}\,\sin(q_1 + q_2).$$

$$\frac{\partial \mathcal{L}}{\partial \dot{q}_2} = m_2 l_{c2}^2 \dot{q}_1 + m_2 l_{c2}^2 \dot{q}_2 + m_2 l_1 l_{c2}\,\cos(q_2)\dot{q}_1 + I_2[\dot{q}_1 + \dot{q}_2].$$

$$\frac{d}{dt}\left[\frac{\partial \mathcal{L}}{\partial \dot{q}_2}\right] = m_2 l_{c2}^2 \ddot{q}_1 + m_2 l_{c2}^2 \ddot{q}_2$$
$$+ m_2 l_1 l_{c2}\,\cos(q_2)\ddot{q}_1 - m_2 l_1 l_{c2}\,\sin(q_2)\dot{q}_1\dot{q}_2$$
$$+ I_2[\ddot{q}_1 + \ddot{q}_2].$$

$$\frac{\partial \mathcal{L}}{\partial q_2} = -m_2 l_1 l_{c2}\,\sin(q_2)\left[\dot{q}_1\dot{q}_2 + \dot{q}_1^2\right] - m_2 g l_{c2}\,\sin(q_1 + q_2).$$

The dynamic equations that model the robot arm are obtained by applying Lagrange's Equations (3.4),

$$\frac{d}{dt}\left[\frac{\partial \mathcal{L}}{\partial \dot{q}_i}\right] - \frac{\partial \mathcal{L}}{\partial q_i} = \tau_i \qquad i = 1, 2$$

from which we finally get

$$\tau_1 = \left[m_1 l_{c1}^2 + m_2 l_1^2 + m_2 l_{c2}^2 + 2m_2 l_1 l_{c2}\,\cos(q_2) + I_1 + I_2\right]\ddot{q}_1$$
$$+ \left[m_2 l_{c2}^2 + m_2 l_1 l_{c2}\,\cos(q_2) + I_2\right]\ddot{q}_2$$
$$- 2m_2 l_1 l_{c2}\,\sin(q_2)\dot{q}_1\dot{q}_2 - m_2 l_1 l_{c2}\,\sin(q_2)\dot{q}_2^2$$
$$+ [m_1 l_{c1} + m_2 l_1]g\,\sin(q_1)$$
$$+ m_2 g l_{c2}\,\sin(q_1 + q_2) \qquad\qquad (5.3)$$

and

$$\tau_2 = \left[m_2 l_{c2}^2 + m_2 l_1 l_{c2}\,\cos(q_2) + I_2\right]\ddot{q}_1 + [m_2 l_{c2}^2 + I_2]\ddot{q}_2$$
$$+ m_2 l_1 l_{c2}\,\sin(q_2)\dot{q}_1^2 + m_2 g l_{c2}\,\sin(q_1 + q_2), \qquad\qquad (5.4)$$

where τ_1 and τ_2, are the external torques delivered by the actuators at joints 1 and 2.

Thus, the dynamic equations of the robot (5.3)-(5.4) constitute a set of two nonlinear differential equations of the state variables $\boldsymbol{x} = [\boldsymbol{q}^T\ \dot{\boldsymbol{q}}^T]^T$, that is, of the form (3.1) .

5.3.2 Model in Compact Form

For control purposes, it is more practical to rewrite the Lagrangian dynamic model of the robot, that is, Equations (5.3) and (5.4), in the compact form (3.18), *i.e.*

$$\underbrace{\begin{bmatrix} M_{11}(\boldsymbol{q}) & M_{12}(\boldsymbol{q}) \\ M_{21}(\boldsymbol{q}) & M_{22}(\boldsymbol{q}) \end{bmatrix}}_{M(\boldsymbol{q})} \ddot{\boldsymbol{q}} + \underbrace{\begin{bmatrix} C_{11}(\boldsymbol{q}, \dot{\boldsymbol{q}}) & C_{12}(\boldsymbol{q}, \dot{\boldsymbol{q}}) \\ C_{21}(\boldsymbol{q}, \dot{\boldsymbol{q}}) & C_{22}(\boldsymbol{q}, \dot{\boldsymbol{q}}) \end{bmatrix}}_{C(\boldsymbol{q}, \dot{\boldsymbol{q}})} \dot{\boldsymbol{q}} + \underbrace{\begin{bmatrix} g_1(\boldsymbol{q}) \\ g_2(\boldsymbol{q}) \end{bmatrix}}_{\boldsymbol{g}(\boldsymbol{q})} = \boldsymbol{\tau},$$

where

$$M_{11}(\boldsymbol{q}) = m_1 l_{c1}^2 + m_2 \left[l_1^2 + l_{c2}^2 + 2 l_1 l_{c2} \cos(q_2) \right] + I_1 + I_2$$
$$M_{12}(\boldsymbol{q}) = m_2 \left[l_{c2}^2 + l_1 l_{c2} \cos(q_2) \right] + I_2$$
$$M_{21}(\boldsymbol{q}) = m_2 \left[l_{c2}^2 + l_1 l_{c2} \cos(q_2) \right] + I_2$$
$$M_{22}(\boldsymbol{q}) = m_2 l_{c2}^2 + I_2$$

$$C_{11}(\boldsymbol{q}, \dot{\boldsymbol{q}}) = -m_2 l_1 l_{c2} \sin(q_2) \dot{q}_2$$
$$C_{12}(\boldsymbol{q}, \dot{\boldsymbol{q}}) = -m_2 l_1 l_{c2} \sin(q_2) \left[\dot{q}_1 + \dot{q}_2 \right]$$
$$C_{21}(\boldsymbol{q}, \dot{\boldsymbol{q}}) = m_2 l_1 l_{c2} \sin(q_2) \dot{q}_1$$
$$C_{22}(\boldsymbol{q}, \dot{\boldsymbol{q}}) = 0$$

$$g_1(\boldsymbol{q}) = \left[m_1 l_{c1} + m_2 l_1 \right] g \sin(q_1) + m_2 l_{c2} g \sin(q_1 + q_2)$$
$$g_2(\boldsymbol{q}) = m_2 l_{c2} g \sin(q_1 + q_2) \,.$$

We emphasize that the appropriate state variables to describe the dynamic model of the robot are the positions q_1 and q_2 and the velocities $\dot{q}_1$ and $\dot{q}_2$. In terms of these state variables, the dynamic model of the robot may be written as

$$\frac{d}{dt} \begin{bmatrix} q_1 \\ q_2 \\ \dot{q}_1 \\ \dot{q}_2 \end{bmatrix} = \begin{bmatrix} \dot{q}_1 \\ \dot{q}_2 \\ M(\boldsymbol{q})^{-1} \left[\boldsymbol{\tau}(t) - C(\boldsymbol{q}, \dot{\boldsymbol{q}}) \dot{\boldsymbol{q}} - \boldsymbol{g}(\boldsymbol{q}) \right] \end{bmatrix}.$$

Properties of the Dynamic Model

We present now the derivation of certain bounds on the inertia matrix, the matrix of centrifugal and Coriolis forces and the vector of gravitational torques. The bounds that we derive are fundamental to properly tune the gains of the controllers studied in the succeeding chapters. We emphasize that, as studied in Chapter 4, some bounds exist for any manipulator with only revolute rigid joints. Here, we show how they can be computed for CICESE's Pelican prototype illustrated in Figure 5.2.

Derivation of $\lambda_{\min}\{M\}$

We start with the property of positive definiteness of the inertia matrix. For a symmetric 2×2 matrix

$$\begin{bmatrix} M_{11}(\boldsymbol{q}) & M_{21}(\boldsymbol{q}) \\ M_{21}(\boldsymbol{q}) & M_{22}(\boldsymbol{q}) \end{bmatrix}$$

to be positive definite for all $\boldsymbol{q} \in \mathbb{R}^n$, it is necessary and sufficient that[2] $M_{11}(\boldsymbol{q}) > 0$ and its determinant

$$M_{11}(\boldsymbol{q})M_{22}(\boldsymbol{q}) - M_{21}(\boldsymbol{q})^2$$

also be positive for all $\boldsymbol{q} \in \mathbb{R}^n$.

In the worst-case scenario $M_{11}(\boldsymbol{q}) = m_1 l_{c1}^2 + I_1 + I_2 + m_2(l_1 - l_{c2})^2 > 0$, we only need to compute the determinant of $M(\boldsymbol{q})$, that is,

$$\det[M(\boldsymbol{q})] = I_1 I_2 + I_2[l_{c1}^2 m_1 + l_1^2 m_2] + l_{c2}^2 m_2 I_1 + l_{c1}^2 l_{c2}^2 m_1 m_2 \\ + l_1^2 l_{c2}^2 m_2^2 [1 - \cos^2(q_2)].$$

Notice that only the last term depends on $\boldsymbol{q}$ and is positive or zero. Hence, we conclude that $M(\boldsymbol{q})$ is positive definite for all $q \in \mathbb{R}^n$, that is[3]

$$\boldsymbol{x}^T M(\boldsymbol{q})\boldsymbol{x} \geq \lambda_{\min}\{M\}\|\boldsymbol{x}\|^2 \tag{5.5}$$

for all $\boldsymbol{q} \in \mathbb{R}^n$, where $\lambda_{\min}\{M\} > 0$.

Inequality (5.5) constitutes an important property for control purposes since for instance, it guarantees that $M(\boldsymbol{q})^{-1}$ is positive definite and bounded for all $\boldsymbol{q} \in \mathbb{R}^n$.

Let us continue with the computation of the constants β, k_M, k_{C_1}, k_{C_2} and k_g from the properties presented in Chapter 4.

Derivation of $\lambda_{\text{Max}}\{M\}$

Consider the inertia matrix $M(\boldsymbol{q})$. From its components it may be verified that

---

[2] Consider the partitioned matrix

$$\begin{bmatrix} A & B \\ B^T & C \end{bmatrix}.$$

If $A = A^T > 0$, $C = C^T > 0$ and $C - B^T A^{-1} B \geq 0$ (resp. $C - B^T A^{-1} B > 0$), then this matrix is positive semidefinite (resp. positive definite). See Horn R. A., Johnson C. R., 1985, *Matrix analysis*, p. 473.

[3] See also Remark 2.1 on page 25.

$$\max_{i,j,\boldsymbol{q}} |M_{ij}(\boldsymbol{q})| = m_1 l_{c1}^2 + m_2 \left[l_1^2 + l_{c2}^2 + 2l_1 l_{c2} \right] + I_1 + I_2 \,.$$

According to Table 4.1, the constant β may be obtained as a value larger or equal to n times the previous expression, *i.e.*

$$\beta \geq n \left[m_1 l_{c1}^2 + m_2 \left[l_1^2 + l_{c2}^2 + 2l_1 l_{c2} \right] + I_1 + I_2 \right] \,.$$

Hence, defining, $\lambda_{\mathrm{Max}}\{M\} = \beta$ we see that

$$\boldsymbol{x}^T M(\boldsymbol{q})\boldsymbol{x} \leq \lambda_{\mathrm{Max}}\{M\}\|\boldsymbol{x}\|^2$$

for all $\boldsymbol{q} \in \mathrm{I\!R}^n$. Moreover, using the numerical values presented in Table 5.1, we get $\beta = 0.7193$ kg m^2, that is, $\lambda_{\mathrm{Max}}\{M\} = 0.7193$ kg m^2.

Derivation of k_M

Consider the inertia matrix $M(\boldsymbol{q})$. From its components it may be verified that

$$\frac{\partial M_{11}(\boldsymbol{q})}{\partial q_1} = 0, \quad \frac{\partial M_{11}(\boldsymbol{q})}{\partial q_2} = -2m_2 l_1 l_{c2}\sin(q_2)$$

$$\frac{\partial M_{12}(\boldsymbol{q})}{\partial q_1} = 0, \quad \frac{\partial M_{12}(\boldsymbol{q})}{\partial q_2} = -m_2 l_1 l_{c2}\sin(q_2)$$

$$\frac{\partial M_{21}(\boldsymbol{q})}{\partial q_1} = 0, \quad \frac{\partial M_{21}(\boldsymbol{q})}{\partial q_2} = -m_2 l_1 l_{c2}\sin(q_2)$$

$$\frac{\partial M_{22}(\boldsymbol{q})}{\partial q_1} = 0, \quad \frac{\partial M_{22}(\boldsymbol{q})}{\partial q_2} = 0 \,.$$

According to Table 4.1, the constant k_M may be determined as

$$k_M \geq n^2 \left(\max_{i,j,k,\boldsymbol{q}} \left| \frac{\partial M_{ij}(\boldsymbol{q})}{\partial q_k} \right| \right) ,$$

hence, this constant may be chosen to satisfy

$$k_M \geq n^2 2m_2 l_1 l_{c2} \,.$$

Using the numerical values presented in Table 5.1 we get $k_M = 0.0974$ kg m^2 .

Derivation of k_{C_1}

Consider the vector of centrifugal and Coriolis forces $C(\boldsymbol{q}, \dot{\boldsymbol{q}})\dot{\boldsymbol{q}}$ written as

$$C(\boldsymbol{q},\dot{\boldsymbol{q}})\dot{\boldsymbol{q}} = \begin{bmatrix} -m_2 l_1 l_{c2} \sin(q_2) \left(2\dot{q}_1 \dot{q}_2 + \dot{q}_2^2 \right) \\[2mm] m_2 l_1 l_{c2} \sin(q_2)\dot{q}_1^2 \end{bmatrix}$$

$$
= \begin{bmatrix} \begin{bmatrix} \dot{q}_1 \\ \dot{q}_2 \end{bmatrix}^T \overbrace{\begin{bmatrix} 0 & -m_2 l_1 l_{c2}\,\sin(q_2) \\ -m_2 l_1 l_{c2}\,\sin(q_2) & -m_2 l_1 l_{c2}\,\sin(q_2) \end{bmatrix}}^{C_1(q)} \begin{bmatrix} \dot{q}_1 \\ \dot{q}_2 \end{bmatrix} \\[2em] \begin{bmatrix} \dot{q}_1 \\ \dot{q}_2 \end{bmatrix}^T \underbrace{\begin{bmatrix} m_2 l_1 l_{c2}\,\sin(q_2) & 0 \\ 0 & 0 \end{bmatrix}}_{C_2(q)} \begin{bmatrix} \dot{q}_1 \\ \dot{q}_2 \end{bmatrix} \end{bmatrix} . \tag{5.6}
$$

According to Table 4.1, the constant k_{C_1} may be derived as

$$
k_{C_1} \geq n^2 \left(\max_{i,j,k,q} |C_{k_{ij}}(q)| \right)
$$

hence, this constant may be chosen so that

$$
k_{C_1} \geq n^2 m_2 l_1 l_{c2}
$$

Consequently, in view of the numerical values from Table 5.1 we find that $k_{C_1} = 0.0487$ kg m^2.

Derivation of k_{C_2}

Consider again the vector of centrifugal and Coriolis forces $C(q, \dot{q})\dot{q}$ written as in (5.6). From the matrices $C_1(q)$ and $C_2(q)$ it may easily be verified that

$$
\frac{\partial C_{1_{11}}(q)}{\partial q_1} = 0, \quad \frac{\partial C_{1_{11}}(q)}{\partial q_2} = 0
$$

$$
\frac{\partial C_{1_{12}}(q)}{\partial q_1} = 0, \quad \frac{\partial C_{1_{12}}(q)}{\partial q_2} = -m_2 l_1 l_{c2}\cos(q_2)
$$

$$
\frac{\partial C_{1_{21}}(q)}{\partial q_1} = 0, \quad \frac{\partial C_{1_{21}}(q)}{\partial q_2} = -m_2 l_1 l_{c2}\cos(q_2)
$$

$$
\frac{\partial C_{1_{22}}(q)}{\partial q_1} = 0, \quad \frac{\partial C_{1_{22}}(q)}{\partial q_2} = -m_2 l_1 l_{c2}\cos(q_2)
$$

$$
\frac{\partial C_{2_{11}}(q)}{\partial q_1} = 0, \quad \frac{\partial C_{2_{11}}(q)}{\partial q_2} = m_2 l_1 l_{c2}\cos(q_2)
$$

$$
\frac{\partial C_{2_{12}}(q)}{\partial q_1} = 0, \quad \frac{\partial C_{2_{12}}(q)}{\partial q_2} = 0
$$

$$
\frac{\partial C_{2_{21}}(q)}{\partial q_1} = 0, \quad \frac{\partial C_{2_{21}}(q)}{\partial q_2} = 0
$$

$$\frac{\partial C_{2_{22}}(\boldsymbol{q})}{\partial q_1} = 0, \ \frac{\partial C_{2_{22}}(\boldsymbol{q})}{\partial q_2} = 0 \,.$$

Furthermore, according to Table 4.1 the constant k_{C_2} may be taken to satisfy

$$k_{C_2} \geq n^3 \left(\max_{i,j,k,l,\boldsymbol{q}} \left| \frac{\partial C_{k_{ij}}(\boldsymbol{q})}{\partial q_l} \right| \right) \,.$$

Therefore, we may choose k_{C_2} as

$$k_{C_2} \geq n^3 m_2 l_1 l_{c2} \,,$$

which, in view of the numerical values from Table 5.1, takes the numerical value $k_{C_2} = 0.0974$ kg m^2:

Derivation of k_g

According to the components of the gravitational torques vector $\boldsymbol{g}(\boldsymbol{q})$ we have

$$\frac{\partial g_1(\boldsymbol{q})}{\partial q_1} = (m_1 l_{c1} + m_2 l_1) \, g \, \cos(q_1) + m_2 l_{c2} g \, \cos(q_1 + q_2)$$

$$\frac{\partial g_1(\boldsymbol{q})}{\partial q_2} = m_2 l_{c2} g \, \cos(q_1 + q_2)$$

$$\frac{\partial g_2(\boldsymbol{q})}{\partial q_1} = m_2 l_{c2} g \, \cos(q_1 + q_2)$$

$$\frac{\partial g_2(\boldsymbol{q})}{\partial q_2} = m_2 l_{c2} g \, \cos(q_1 + q_2) \,.$$

Notice that the Jacobian matrix $\dfrac{\partial \boldsymbol{g}(\boldsymbol{q})}{\partial \boldsymbol{q}}$ corresponds in fact, to the Hessian matrix (*i.e.* the second partial derivative) of the potential energy function $\mathcal{U}(\boldsymbol{q})$, and is a symmetric matrix even though not necessarily positive definite.

The positive constant k_g may be derived from the information given in Table 4.1 as

$$k_g \geq n \ \max_{i,j,\boldsymbol{q}} \left| \frac{\partial g_i(\boldsymbol{q})}{\partial q_j} \right| \,.$$

That is,

$$k_g \geq n \left[m_1 l_{c1} + m_2 l_1 + m_2 l_{c2} \right] g$$

and using the numerical values from Table 5.1 may be given the numerical value $k_g = 23.94$ kg m^2/s^2.

Table 5.2. Numeric values of the parameters for the CICESE prototype

Parameter	Value	Units
$\lambda_{\mathrm{Max}}\{M\}$	0.7193	kg m^2
k_M	0.0974	kg m^2
k_{C_1}	0.0487	kg m^2
k_{C_2}	0.0974	kg m^2
k_g	23.94	kg m^2/s^2

Summary

The numerical values of the constants $\lambda_{\mathrm{Max}}\{M\}$, k_M, k_{C_1}, k_{C_2} and k_g obtained above are summarized in Table 5.2.

5.4 Desired Reference Trajectories

With the aim of testing in experiments the performance of the controllers presented in this book, on the Pelican robot, we have selected the following reference trajectories in *joint space*:

$$\begin{bmatrix} q_{d1} \\ q_{d2} \end{bmatrix} = \begin{bmatrix} b_1[1 - e^{-2.0\ t^3}] + c_1[1 - e^{-2.0\ t^3}]\sin(\omega_1 t) \\ b_2[1 - e^{-2.0\ t^3}] + c_2[1 - e^{-2.0\ t^3}]\sin(\omega_2 t) \end{bmatrix} \quad \text{[rad]} \qquad (5.7)$$

where $b_1 = \pi/4$ [rad], $c_1 = \pi/9$ [rad] and $\omega_1 = 4$ [rad/s], are parameters for the desired position reference for the first joint and $b_2 = \pi/3$ [rad], $c_2 = \pi/6$ [rad] and $\omega_2 = 3$ [rad/s] correspond to parameters that determine the desired position reference for the second joint. Figure 5.5 shows graphs of these reference trajectories against time.

Note the following important features in these reference trajectories:

- the trajectory contains a sinusoidal term to evaluate the performance of the controller following relatively fast periodic motions. This test is significant since such motions excite nonlinearities in the system.
- It also contains a slowly increasing term to bring the robot to the operating point without driving the actuators into saturation.

The module and frequency of the periodic signal must be chosen with care to avoid both torque and speed saturation in the actuators. In other
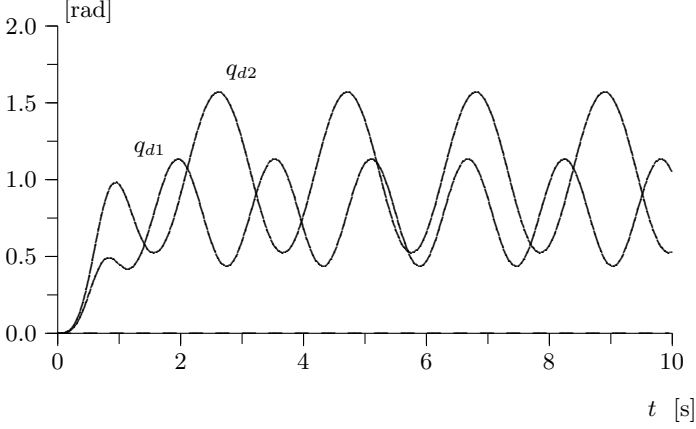
Figure 5.5. Desired reference trajectories

words, the reference trajectories must be such that the evolution of the robot dynamics along these trajectories gives admissible velocities and torques for the actuators. Otherwise, the desired reference is physically unfeasible.

Using the expressions of the desired position trajectories, (5.7), we may obtain analytically expressions for the desired velocity reference trajectories. These are obtained by direct differentiation, *i.e.*

$$\dot{q}_{d1} = 6b_1 t^2 e^{-2.0\ t^3} + 6c_1 t^2 e^{-2.0\ t^3} \sin(\omega_1 t) + [c_1 - c_1 e^{-2.0\ t^3}] \cos(\omega_1 t)\omega_1,$$

$$\dot{q}_{d2} = 6b_2 t^2 e^{-2.0\ t^3} + 6c_2 t^2 e^{-2.0\ t^3} \sin(\omega_2 t) + [c_2 - c_2 e^{-2.0\ t^3}] \cos(\omega_2 t)\omega_2,$$

$$(5.8)$$

in $[\mathrm{rad/s}]$. In the same way we may proceed to compute the reference accelerations to obtain
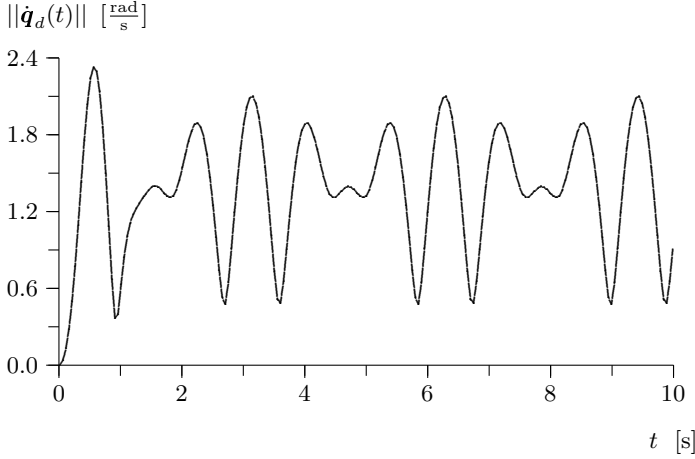
$$
\begin{aligned}
\ddot{q}_{d1} = {} & 12b_1 t e^{-2.0\ t^3} - 36b_1 t^4 e^{-2.0\ t^3} + 12c_1 t e^{-2.0\ t^3} \sin(\omega_1 t) \\
& - 36c_1 t^4 e^{-2.0\ t^3} \sin(\omega_1 t) + 12c_1 t^2 e^{-2.0\ t^3} \cos(\omega_1 t)\omega_1 \\
& - [c_1 - c_1 e^{-2.0\ t^3}] \sin(\omega_1 t)\omega_1^2 \quad [\mathrm{rad/s^2}],
\end{aligned}
$$

$$
\begin{aligned}
\ddot{q}_{d2} = {} & 12b_2 t e^{-2.0\ t^3} - 36b_2 t^4 e^{-2.0\ t^3} + 12c_2 t e^{-2.0\ t^3} \sin(\omega_2 t) \\
& - 36c_2 t^4 e^{-2.0\ t^3} \sin(\omega_2 t) + 12c_2 t^2 e^{-2.0\ t^3} \cos(\omega_2 t)\omega_2 \\
& - [c_2 - c_2 e^{-2.0\ t^3}] \sin(\omega_2 t)\omega_2^2 \quad [\mathrm{rad/s^2}].
\end{aligned}
$$

$$(5.9)$$

$||\boldsymbol{q}_d(t)||$ [rad]
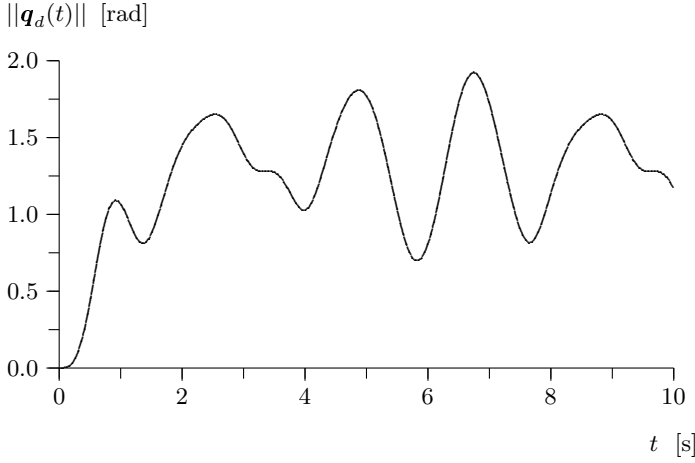
Figure 5.6. Norm of the desired positions

$||\dot{\boldsymbol{q}}_d(t)||$ $[\frac{\text{rad}}{\text{s}}]$

Figure 5.7. Norm of the desired velocities vector

Figures 5.6, 5.7 and 5.8 show the evolution in time of the norms corresponding to the desired joint positions, velocities and accelerations respectively. From these figures we deduce the following upper-bounds on the norms

$$\|\boldsymbol{q}_d\|_{\text{Max}} \leq 1.92 \; [\text{rad}]$$
$$\|\dot{\boldsymbol{q}}_d\|_{\text{Max}} \leq 2.33 \; [\text{rad/s}]$$
$$\|\ddot{\boldsymbol{q}}_d\|_{\text{Max}} \leq 9.52 \; [\text{rad/s}^2] \,.$$
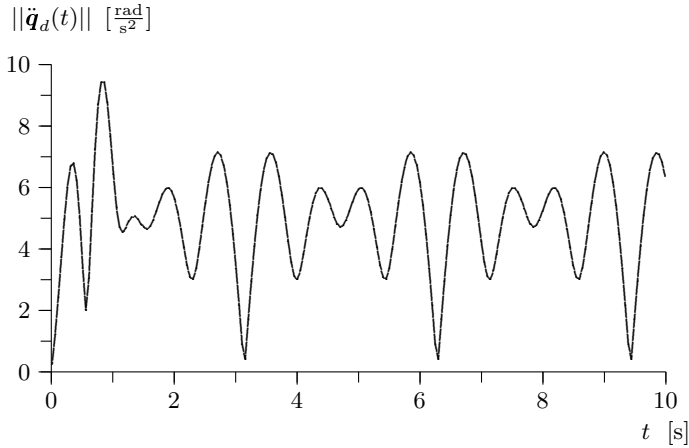
Figure 5.8. Norm of the desired accelerations vector

Bibliography

The schematic diagram of the robot depicted in Figure 5.2 and elsewhere throughout the book, corresponds to a real experimental prototype robot arm designed and constructed in the CICESE Research Center, Mexico[4].

The numerical values that appear in Table 5.1 are taken from:

- Campa R., Kelly R., Santibáñez V., 2004, *"Windows-based real-time control of direct-drive mechanisms: platform description and experiments"*, Mechatronics, Vol. 14, No. 9, pp. 1021–1036.

The constants listed in Table 5.2 may be computed based on data reported in

- Moreno J., Kelly R., Campa R., 2003, *"Manipulator velocity control using friction compensation"*, IEE Proceedings - Control Theory and Applications, Vol. 150, No. 2.

Problems

1. Consider the matrices $M(\boldsymbol{q})$ and $C(\boldsymbol{q}, \dot{\boldsymbol{q}})$ from Section 5.3.2. Show that the matrix $\left[\frac{1}{2}\dot{M}(\boldsymbol{q}) - C(\boldsymbol{q}, \dot{\boldsymbol{q}})\right]$ is skew-symmetric.

2. According to Property 4.2, the centrifugal and Coriolis forces matrix $C(\boldsymbol{q}, \dot{\boldsymbol{q}})$, of the dynamic model of an n-DOF robot is not unique. In Section 5.3.2 we computed the elements of the matrix $C(\boldsymbol{q}, \dot{\boldsymbol{q}})$ of the Pelican

---

[4] "Centro de Investigación Científica y de Educación Superior de Ensenada".

robot presented in this chapter. Prove also that the matrix $C(\boldsymbol{q}, \dot{\boldsymbol{q}})$ whose elements are given by

$$C_{11}(\boldsymbol{q}, \dot{\boldsymbol{q}}) = -2m_2 l_1 l_{c2} \, \sin(q_2)\dot{q}_2$$
$$C_{12}(\boldsymbol{q}, \dot{\boldsymbol{q}}) = -m_2 l_1 l_{c2} \, \sin(q_2)\dot{q}_2$$
$$C_{21}(\boldsymbol{q}, \dot{\boldsymbol{q}}) = m_2 l_1 l_{c2} \, \sin(q_2)\dot{q}_1$$
$$C_{22}(\boldsymbol{q}, \dot{\boldsymbol{q}}) = 0$$

characterizes the centrifugal and Coriolis forces, $C(\boldsymbol{q}, \dot{\boldsymbol{q}})\dot{\boldsymbol{q}}$. With this definition of $C(\boldsymbol{q}, \dot{\boldsymbol{q}})$, is $\frac{1}{2}\dot{M}(\boldsymbol{q}) - C(\boldsymbol{q}, \dot{\boldsymbol{q}})$ skew-symmetric?

Does it hold that $\dot{\boldsymbol{q}}^T \left[\frac{1}{2}\dot{M}(\boldsymbol{q}) - C(\boldsymbol{q}, \dot{\boldsymbol{q}}) \right] \dot{\boldsymbol{q}} = 0$? Explain.

Springer